

25. *Earthquake Generating Stress in Japan
for the Years 1961 to 1963
Obtained by Smoothing the First Motion Radiation Patterns.*

By Keiiti AKI,

Earthquake Research Institute.

(Read Dec. 21, 1965.—Received March 30, 1966.)

§ 1. Introduction

In the statistical discussions^{1),2),3),4),5)} of regional earthquake generating stress based on the first motion studies, average orientation of some axes of tectonic significance is obtained visually or analytically from fault plane solutions of individual earthquakes in the region. This method is applicable to large earthquakes for which enough data assure the uniqueness of the individual solutions. For small earthquakes without sufficient data, however, the individual solutions may be biased according to arbitrary or prejudiced presumptions of the investigators. Thus, it is not impossible that the averaged solution may be but an averaged presumption rather than an averaged observation.

An alternative method^{6),7)} for investigating an average stress pattern is to determine a single solution for a group of earthquakes by the superposition of the distribution of first motions regarded as if they were coming from a single earthquake. In the present paper, we shall follow this line of approach and obtain averaged radiation patterns for earthquakes with magnitudes down to 4.5 occurring in various parts of Japan in the years 1961 to 1963. We believe that our method minimizes the biasing mentioned above, and determines a short-term average generating-stress pattern objectively.

Such a method applicable to small earthquakes is useful in a de-

1) H. HONDA, *Geophys. Notes*, **15** (1962), Supplement.

2) M. ICHIKAWA, *Geophys. Mag.*, **30** (1960), 355-403.

3) J. H. HODGSON, *Bull. Geol. Soc. Am.*, **68** (1957), 611-644.

4) H. D. FARA and A. E. SCHEIDEGGER, *Bull. Seis. Soc. Am.*, **53** (1963), 811-816.

5) A. R. RITSEMA, *Publ. Dominion Obs. Ottawa*, **24** (1960), 355-358.

6) B. GUTENBERG, *Bull. Seis. Soc. Am.*, **31** (1941), 263-302.

7) T. HAGIWARA, S. MURAUCHI and J. YAMADA, *Sp. Rep. Earthq. Res. Inst.*, No. 5 (1947), 164.

Table 1. List of earthquakes.

Area	Year	Month	Date	Origin time (JST)	Latitude (deg.)	Longitude (deg.)	Depth (km)	Magni- tude	Number of push-pull	Total number (each area)	Crustal thickness (km)
1	1961	Aug.	7	13:02:19.6	42.10	142.15	35	4.9	6	36	29
	1962	Nov.	13	17:54:41.1	41.98	142.22	68	5.0	6		29
	1962	Dec.	21	18:33:19.6	42.00	142.50	74	6.3	16		29
2	1963	May	17	21:09:07.2	41.49	142.14	69	5.4	8	58	29
	1961	May	27	19:23:07.9	38.73	141.79	80	5.0	10		27
	1961	Sept.	15	06:50:44.4	37.54	141.88	65	5.0	9		27
	1961	Dec.	29	14:40:46.6	37.47	141.72	0	4.5	3		27
	1962	July	30	19:51:05.6	39.35	142.04	43	4.9	7		27
	1962	Oct.	15	06:13:42.4	38.59	141.97	56	4.7	10		27
	1962	Oct.	23	07:18:47.2	37.55	142.03	40	4.8	11		27
	1963	Apr.	5	09:51:51.1	38.45	142.37	40	4.9	8		27
	1961	Mar.	9	18:12:40.4	38.34	141.11	86	—	7		27
	1961	Apr.	9	04:18:53.2	37.92	140.73	139	—	7		27
3	1962	July	15	15:47:22.5	39.51	141.29	104	—	11	32	27
	1962	July	20	07:05:49.1	39.45	141.11	66	—	7		27
	1961	Jan.	16	23:44:09.2	36.36	141.67	7	5.5	7		27
	1961	Jan.	21	07:34:46.9	37.07	141.66	49	5.5	7		27
	1961	Feb.	3	22:31:42.4	36.38	141.15	22	5.4	7		27
	1961	Mar.	19	18:18:47.1	36.63	141.26	49	5.3	7		27
	1961	Mar.	30	03:10:19.7	36.85	141.52	28	5.4	8		27
	1961	July	4	08:14:23.8	36.67	141.10	94	—	10		27
	1961	Sept.	2	18:03:53.5	36.83	140.95	64	4.5	5		27
	1961	Nov.	20	13:32:34.4	37.05	141.52	49	5.1	11		27
4	1961	Dec.	19	23:31:14.6	37.16	141.62	15	4.6	4	162	27
	1962	June	1	06:43:44.9	37.08	141.08	49	4.6	7		27
	1962	June	23	13:23:43.0	37.04	141.19	51	4.8	8		27
	1962	Aug.	9	02:55:36.3	37.07	141.57	40	4.9	10		27
	1963	Mar.	21	13:00:10.4	36.35	141.19	25	5.4	17		29
	1963	May	8	19:22:08.7	36.40	141.28	16	6.1	24		29
	1963	May	12	11:57:18.2	36.45	141.10	14	4.6	10		29
	1963	May	23	19:43:28.6	36.29	141.18	23	4.5	10		29
	1963	May	25	06:00:21.4	36.31	141.23	23	4.7	10		29
	1961	July	4	23:31:07.7	35.85	140.58	30	4.4	11		32

(to be continued)

(continued)

Area	Year	Month	Date	Origin time (JST)	Latitude (deg.)	Longitude (deg.)	Depth (km)	Magnitude	Number of push-pull	Total number (each area)	Crustal thickness (km)		
6	1961	Nov.	29	01:37:52.7	35.62	140.61	46	5.0	6	70	32		
	1962	Jan.	16	07:59:44.1	35.74	140.60	28	4.5	8		32		
	1962	Feb.	9	10:01:44.8	35.67	141.08	67	4.7	7		32		
	1962	Nov.	14	16:48:04.7	35.80	141.08	34	5.8	22		32		
	1962	Nov.	15	22:48:31.3	35.64	140.97	76	4.8	9		32		
	1963	May	29	06:58:20.6	35.40	141.08	26	4.9	7		32		
	1961	Feb.	26	00:23:08.1	35.95	139.73	39	4.8	6		32		
	1961	June	8	10:11:58.0	35.77	140.14	79	—	8		32		
	1961	June	23	20:04:58.6	35.73	140.14	71	—	17		32		
	1961	July	14	08:41:33.7	36.03	139.90	55	4.7	6		32		
	1961	Sept.	3	00:38:25.3	35.80	140.17	81	—	11		32		
	1961	Sept.	14	08:17:23.6	36.13	140.11	65	4.6	5		32		
	1962	Jan.	30	02:46:19.0	36.06	139.81	120	—	8		33		
	1962	Apr.	23	12:54:40.5	36.18	139.94	50	5.1	9		32		
	1962	May	15	00:19:06.7	36.08	139.86	71	4.8	4		32		
1962	Oct.	24	07:27:56.8	35.91	140.15	70	—	8	32				
1962	Nov.	9	18:21:35.6	35.94	140.47	50	5.4	15	32				
1963	Jan.	11	14:02:03.7	35.97	140.44	71	4.4	13	32				
1963	Mar.	22	11:38:45.7	36.19	139.84	66	4.7	11	121	33			
7	1961	Nov.	14	19:02:28.5	35.44	139.35	158	—	21	58	37		
	1962	Jan.	4	13:16:05.2	35.07	139.28	135	—	15		37		
	1962	Feb.	6	07:55:54.0	35.88	139.30	117	—	22		37		
	1961	Jan.	2	12:39:15.9	35.58	138.75	17	—	6		37		
	1961	Feb.	17	22:31:36.0	35.51	139.01	12	4.9	13		37		
	1961	Sept.	2	03:59:33.4	35.46	139.16	5	5.0	12		37		
8	1961	Dec.	15	02:24:21.0	35.34	139.28	0	4.4	8	59	37		
	1961	Dec.	15	02:53:12.0	35.34	139.26	0	4.6	10		37		
	1962	Dec.	31	02:56:27.2	35.47	139.12	9	4.6	10		37		
	1961	Feb.	16	17:55:06.5	33.80	137.64	362	—	14		32		
	1961	Dec.	24	04:12:00.6	34.83	138.21	201	—	8		37		
	1962	May	6	01:42:58.7	35.81	137.27	305	—	5		37		
	1962	Oct.	17	21:39:11.1	33.34	138.09	351	—	12		32		
	1962	Dec.	9	08:15:27.1	37.17	138.59	187	—	6		37		
	9	1961	Nov.	29	01:37:52.7	35.62	140.61	46	5.0		6	70	32
		1962	Jan.	16	07:59:44.1	35.74	140.60	28	4.5		8		32
1962		Feb.	9	10:01:44.8	35.67	141.08	67	4.7	7	32			
1962		Nov.	14	16:48:04.7	35.80	141.08	34	5.8	22	32			
1962		Nov.	15	22:48:31.3	35.64	140.97	76	4.8	9	32			
1963		May	29	06:58:20.6	35.40	141.08	26	4.9	7	32			
1961		Feb.	26	00:23:08.1	35.95	139.73	39	4.8	6	32			
1961		June	8	10:11:58.0	35.77	140.14	79	—	8	32			
1961		June	23	20:04:58.6	35.73	140.14	71	—	17	32			
1961		July	14	08:41:33.7	36.03	139.90	55	4.7	6	32			
1961		Sept.	3	00:38:25.3	35.80	140.17	81	—	11	32			
1961		Sept.	14	08:17:23.6	36.13	140.11	65	4.6	5	32			
1962		Jan.	30	02:46:19.0	36.06	139.81	120	—	8	33			
1962		Apr.	23	12:54:40.5	36.18	139.94	50	5.1	9	32			
1962		May	15	00:19:06.7	36.08	139.86	71	4.8	4	32			
1962	Oct.	24	07:27:56.8	35.91	140.15	70	—	8	32				
1962	Nov.	9	18:21:35.6	35.94	140.47	50	5.4	15	32				
1963	Jan.	11	14:02:03.7	35.97	140.44	71	4.4	13	32				
1963	Mar.	22	11:38:45.7	36.19	139.84	66	4.7	11	121	33			
1961	Nov.	14	19:02:28.5	35.44	139.35	158	—	21	21	37			
1962	Jan.	4	13:16:05.2	35.07	139.28	135	—	15	15	37			
1962	Feb.	6	07:55:54.0	35.88	139.30	117	—	22	22	37			
1961	Jan.	2	12:39:15.9	35.58	138.75	17	—	6	6	37			
1961	Feb.	17	22:31:36.0	35.51	139.01	12	4.9	13	13	37			
1961	Sept.	2	03:59:33.4	35.46	139.16	5	5.0	12	12	37			
1961	Dec.	15	02:24:21.0	35.34	139.28	0	4.4	8	8	37			
1961	Dec.	15	02:53:12.0	35.34	139.26	0	4.6	10	10	37			
1962	Dec.	31	02:56:27.2	35.47	139.12	9	4.6	10	10	37			
1961	Feb.	16	17:55:06.5	33.80	137.64	362	—	14	14	32			
1961	Dec.	24	04:12:00.6	34.83	138.21	201	—	8	8	37			
1962	May	6	01:42:58.7	35.81	137.27	305	—	5	5	37			
1962	Oct.	17	21:39:11.1	33.34	138.09	351	—	12	12	32			
1962	Dec.	9	08:15:27.1	37.17	138.59	187	—	6	6	37			

(to be continued)

(continued)

Area	Year	Month	Date	Origin time (JST)	Latitude (deg.)	Longitude (deg.)	Depth (km)	Magni- tude	Number of push-pull (each area)	Total number (each area)	Crustal thickness (km)
10	1963	Jan.	18	12:12:03.9	33.23	135.94	474	—	18	63	32
	1961	July	6	20:23:40.3	35.54	138.32	0	—	6		37
	1961	Aug.	19	22:24:13.0	36.51	137.65	0	4.9	8		37
	1961	Oct.	25	18:49:28.8	35.00	138.35	14	—	5		37
	1962	May	27	14:37:28.3	36.15	137.54	0	4.8	11		37
	1962	June	30	03:54:11.6	35.59	137.77	10	4.7	10		37
	1963	Feb.	9	12:53:03.0	36.30	137.71	0	5.5	19	59	35
	1961	Aug.	19	14:33:32.7	36.08	136.74	0	7.0	27		37
	1961	Aug.	19	15:25:46.4	35.99	136.81	0	4.6	3		37
	1961	Aug.	19	17:07:16.3	36.01	136.54	0	5.2	13		37
11	1962	Mar.	5	16:32:32.5	35.70	136.60	3	4.4	7		37
	1962	Apr.	1	13:45:47.1	35.60	137.14	6	4.3	5		37
	1962	May	11	00:09:48.3	36.72	136.49	15	4.8	4	59	37
	1963	Mar.	27	06:34:38.8	35.81	135.78	6	6.9	43		32
	1963	Mar.	27	12:27:47.1	35.80	135.80	0	5.2	17		32
	1963	Mar.	27	15:49:21.6	35.78	135.78	20	5.3	13		32
	1963	Mar.	28	01:13:14.0	35.73	135.78	0	5.2	10	83	32
	1961	Apr.	12	06:44:04.8	34.82	134.52	29	4.5	4		32
	1961	Apr.	18	05:42:33.9	35.00	134.50	7	4.5	8		32
	1961	May	7	21:14:17.2	35.04	134.53	14	5.9	24		32
13	1961	May	7	21:19:59.9	35.00	134.51	14	5.2	12		32
	1961	May	7	00:08:09.4	35.04	134.49	28	4.6	12		32
	1961	Oct.	15	05:38:59.3	34.53	134.86	18	4.7	9	69	32
	1962	Apr.	25	00:08:09.4	34.53	134.86	18	4.7	9		32
	1961	Sept.	1	17:20:56.8	33.88	135.06	15	4.5	13		32
	1962	Mar.	21	00:39:25.9	33.74	135.09	62	4.9	16		32
	1962	July	23	20:25:17.1	33.83	135.02	58	4.4	10		32
	1962	Sept.	8	13:39:37.3	33.78	135.02	59	4.6	12		32
	1963	Jan.	9	00:14:19.9	33.62	134.83	9	4.4	8	59	32
	1961	Feb.	27	03:10:50.9	31.67	131.71	31	7.0	26		29
14	1962	July	31	14:09:23.1	32.40	132.00	58	5.4	10	43	29
	1962	Oct.	15	00:08:58.5	31.67	131.97	2	5.4	7		29
	1961	Nov.	27	14:57:12.5	31.25	131.25	105	6.0	10		29
	1962	Apr.	23	04:15:31.2	32.14	130.78	186	—	13		29
	1963	Jan.	9	00:46:43.2	31.06	130.35	183	—	11	34	29

tailed study of the distribution of earthquake generating stress in space and time, and may be most effectively used for processing micro-earthquake data in a research related to prediction of large earthquakes.

§ 2. Data

The source of data used in the present investigation is the *Monthly Seismological Bulletins* of the Japan Meteorological Agency (JMA) over a 30 month's period from January 1961 to June 1963. First, we selected earthquakes for which enough *ip* readings are reported to permit a reliable redetermination, on the basis of a revised crust-mantle structure, of focal depths and epicentres. We omitted earthquakes which are located in the ocean beyond 100 km from the coast, and those located to the east of Hokkaido or south of Kyushu, because of their greater

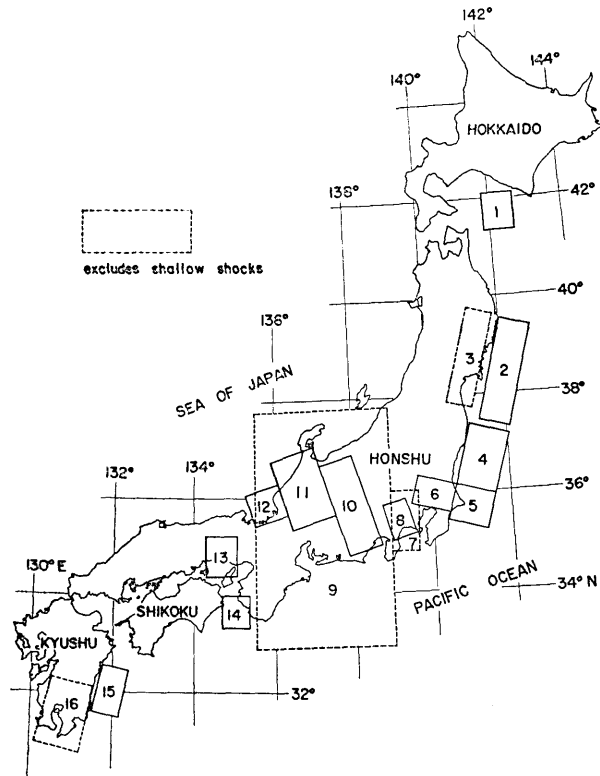


Fig. 1. Map of the area of earthquake group. The radiation patterns of first motions from earthquakes which occurred within each area are superposed and smoothed as shown in Fig. 4 through Fig. 19.

uncertainty in focal depth and also of poor azimuthal coverage of stations around the epicentre. The largest earthquake omitted by such a criterion is the one which occurred in the ocean to the south-east of Hokkaido ($M=7.0$) on April 23, 1962.

Redetermined hypocentres are plotted on a map and divided into 16 groups according to their positions. A few earthquakes are omitted in this grouping, because of their isolated locations. The list of grouped earthquakes is shown in Table 1, and the area of each group is indicated on a map in Fig. 1.

Table 1 lists the origin time, epicentre and focal depth redetermined by the method described in the next section, and the magnitude of earthquake determined by JMA. The number of stations reporting the sign of ip is also shown for each earthquake and for each group of earthquakes. The total number of earthquakes listed is 100, and the total number of the signs of ip is 1065. These numbers are distributed over the earthquake magnitude range from 4.3 to 7.0 in such a manner as shown Table 2. We see that more than 80% of first motion data

Table 2. Distribution of numbers of earthquakes and push-pulls used in the analysis.

Magnitude	Number of earthquakes	Number of push-pulls
4.0-4.9	45	377
5.0-5.9	25	286
6.0-6.9	4	93
7.0	2	52
unknown	24	257
Total	100	1065

are from earthquakes with magnitudes smaller than 6.0.

Major earthquakes in our list are the Hyuganada earthquake ($M=7.0$) of Feb. 27, 1961, the Kitamino earthquake ($M=7.0$) of Aug. 19, 1961 and the Echizenmisaki earthquake ($M=6.9$) of March 27, 1963. All the other earthquakes in our list have magnitudes smaller than 6.4. No earthquakes with magnitude greater than 7.0 took place in Japan during the 30 month's period.

§ 3. Determination of the emergence angle

Determination of the emergence angle of the ray at an earthquake focus for waves which show up as the first arrival at a local station critically depends on the focal depth and the crust-mantle structure in the area.^{8),9)} In the present paper, we determined the focal depth on the basis of the best available crust-mantle model using the arrival times of *ip* reported in the *Seismological Bulletins* of JMA. The emergence angles are computed by the use of the revised focal depth and crust-mantle structure. All these computations are made by a program¹⁰⁾ designed by the present writer for IBM 7090.

The wave medium in our computer program consists of a crust with velocity distribution $v=v_0(r/r_0)^{20}$ and upper mantle with velocity distribution $v=v_1(r/r_1)^{21}$, where r is the distance from the earth's centre. As shown in a previous paper,¹¹⁾ the parameters for the crust are determined to agree with the observed arrival times of *P* waves from the artificial explosions, and those for the upper mantle which fit the Jeffreys-Bullen travel times. We used the following values for all our earthquakes,

$$\begin{aligned}v_0 &= 5.78 \text{ km/sec,} \\r_0 &= 6356.8 \text{ km,} \\z_0 &= -24.4, \\v_1 &= 7.75 \text{ km/sec,} \\z_1 &= -2.3.\end{aligned}$$

Different values of crustal thickness, r_0-r_1 , are used for different earthquakes, according to the position of epicentre and the distribution of relevant stations on a map of crustal thickness obtained from the phase velocity of Rayleigh waves.¹²⁾ The crustal thickness adopted for each earthquake is listed in the last column of Table 1.

The computer output includes, among others, the azimuth to each station, the emergence angle e , and $\tan \{(\pi/2-|e|)/2\}$ for use in the projection of the focal sphere. The signs of first motions on the *upper* focal hemi-sphere of each earthquake are plotted by the stereographic

8) K. WADATI, *Geophys. Mag.*, **1** (1927), 89-96.

9) H. KAWASUMI, *Bull. Earthq. Res. Inst.*, **12** (1934), 660-705.

10) K. AKI, *Bull. Earthq. Res. Inst.*, **43** (1965), 15-22.

11) K. AKI, *Bull. Earthq. Res. Inst.*, **43** (1965), 23-38.

12) K. KAMINUMA, *Bull. Earthq. Res. Inst.*, **42** (1964), 19-38.

projection (Wulff's net). The station for which the emergence angle is negative (ray leaves from the focus toward the centre of the earth) is plotted in the opposite azimuth, assuming that the radiation pattern is symmetric with respect to the focal point. The plot of the first motions is, then, superposed for all the earthquakes belonging to each group.

§ 4. Smoothing on the focal sphere

The distribution of signs of first motions superposed on a focal hemi-sphere is smoothed and normalized by the following procedure.

On the surface of a focal sphere, we take a point Q with azimuth φ and plunge δ and its antipode Q' . (φ is measured clockwise from north, δ measured upward from the horizon). Then, the number N_- of compressions and the number N_+ of dilatations within an angular distance of 45° from the point Q and Q' are counted. For counting these numbers, we use a set of figures which show the area within an angular distance of 45° from a point Q and its antipode Q' on a hemispherical surface as projected by the stereographic projection. Such figures are shown in Fig. 2 for the cases in which the plunge δ of Q is $0, 20^\circ, 40^\circ, 60^\circ$ and 80° .

From the numbers N_+ and N_- for a given point Q , we form a normalized parameter k by the following formula.

$$k = \frac{N_+ - N_-}{N_+ + N_-}.$$

This value takes $+1$ if all the first motions within the area are dilatations, and takes -1 if all of them are compressions. The parameter k is determined for many points Q covering the surface of the focal sphere. Then, the value of k is plotted at the corresponding point Q on a projection of the focal sphere, where the radial distance is equal to the angle from the vertical, and smooth lines of equal k are drawn as shown in Fig. 3. The values of k for the 16 groups of earthquakes are given in Table 3, and the corresponding smoothed lines of equal k are shown in Fig. 4 to Fig. 19. Solid lines are used for positive k and dashed lines for negative k throughout these figures. (The open and closed circles shown in these figures indicate the points where the magnitude of k value is significantly great; see Appendix.)

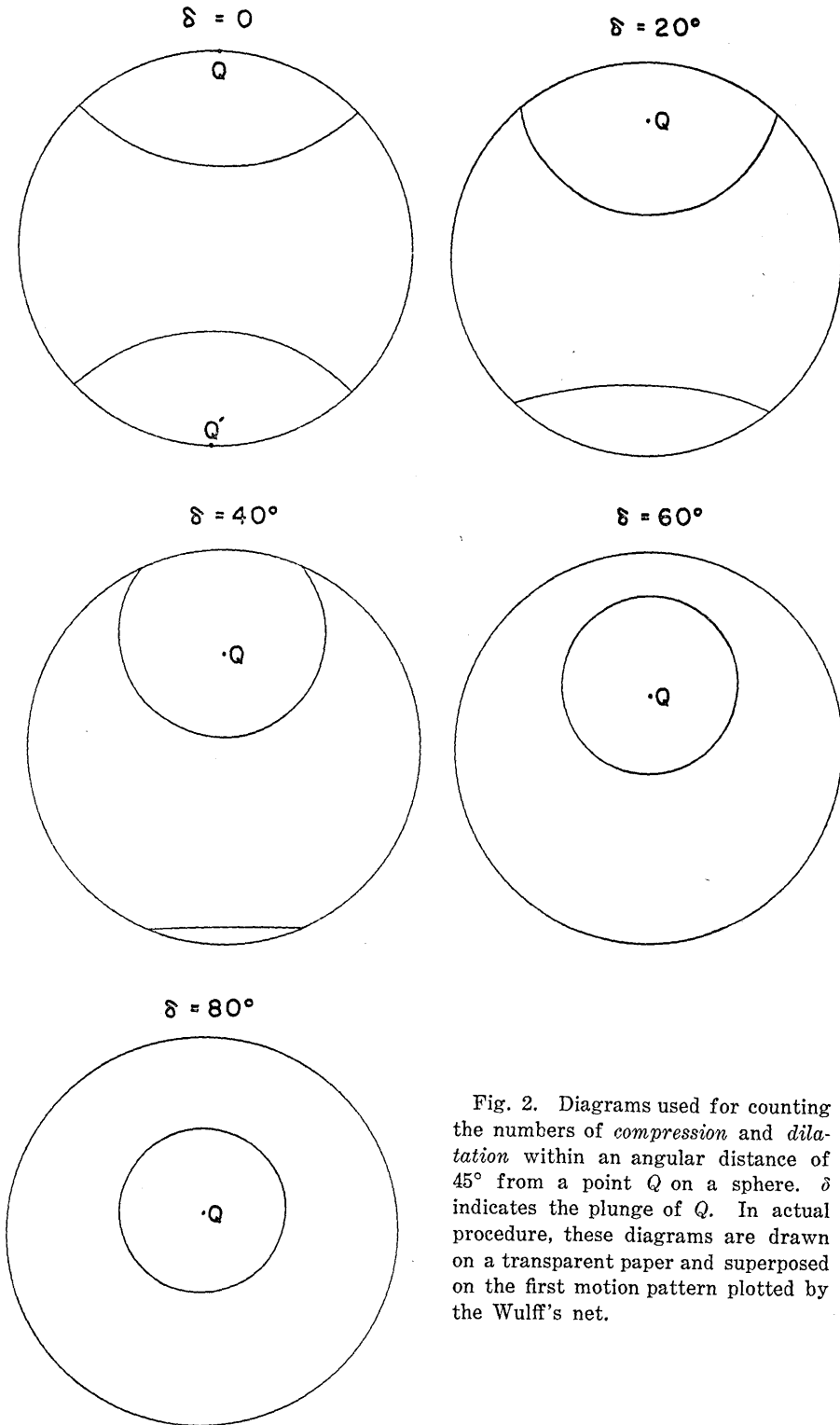


Fig. 2. Diagrams used for counting the numbers of *compression* and *dilatation* within an angular distance of 45° from a point Q on a sphere. δ indicates the plunge of Q . In actual procedure, these diagrams are drawn on a transparent paper and superposed on the first motion pattern plotted by the Wulff's net.

Table 3. The numbers N_+ (dilatation) and N_- (compression) within an angular

Area		1			2			3			4		
δ	φ	N_+	N_-	k	N_+	N_-	k	N_+	N_-	k	N_+	N_-	k
0	0	6	15	-.43	14	13	.04	13	6	.37	41	20	.34
0	20	9	15	-.25	16	12	.14	13	6	.37	35	19	.30
0	40	9	16	-.28	18	12	.20	8	4	.33	36	16	.38
0	60	9	14	-.22	17	13	.13	4	2	.33	55	15	.57
0	80	11	5	.38	19	9	.36	1	0	1.00	66	11	.72
0	100	9	1	.80	16	7	.39	1	0	1.00	53	10	.68
0	120	9	1	.80	15	8	.30	0	0	/	52	11	.65
0	140	8	0	1.00	17	8	.36	1	2	-.33	42	14	.50
0	160	7	8	-.07	14	11	.12	9	5	.29	45	17	.45
20	0	7	13	-.30	13	10	.13	8	5	.23	25	16	.22
20	20	8	16	-.33	16	10	.23	8	5	.23	38	18	.36
20	40	9	17	-.31	15	9	.25	6	3	.33	45	15	.50
20	60	9	11	-.10	16	9	.28	4	0	1.00	59	15	.59
20	80	6	5	.09	13	5	.44	2	0	1.00	63	10	.73
20	100	7	2	.56	10	3	.54	2	0	1.00	62	10	.72
20	120	7	1	.75	11	4	.47	1	0	1.00	62	10	.72
20	140	6	0	1.00	12	6	.33	5	0	1.00	57	13	.63
20	160	5	7	-.17	8	9	-.06	10	2	.67	47	17	.47
20	180	5	12	-.41	11	12	-.04	12	5	.41	46	19	.42
20	200	7	14	-.33	14	16	-.07	13	3	.63	37	19	.32
20	220	9	14	-.22	15	14	.03	11	4	.47	32	16	.33
20	240	9	12	-.14	18	14	.13	5	4	.11	35	13	.46
20	260	11	5	.38	20	10	.33	1	2	-.33	35	9	.59
20	280	9	1	.80	15	9	.25	0	1	-1.00	32	9	.56
20	300	9	0	1.00	15	8	.30	0	2	-1.00	34	10	.55
20	320	8	0	1.00	18	8	.38	0	4	-1.00	33	12	.47
20	340	8	4	.33	15	9	.25	6	4	.20	27	14	.32
40	0	6	5	.09	11	7	.22	6	5	.09	29	15	.32
40	20	6	12	-.33	6	6	0	8	5	.23	28	16	.27
40	40	7	12	-.26	7	3	.40	7	3	.40	35	14	.43
40	60	5	8	-.23	7	2	.56	7	2	.56	42	11	.58
40	80	5	4	.11	5	0	1.00	4	1	.60	47	11	.62
40	100	2	3	-.20	3	0	1.00	3	0	1.00	48	11	.63
40	120	0	3	-1.00	4	1	.60	4	0	1.00	47	10	.65
40	140	1	0	1.00	3	2	.20	7	1	.75	43	11	.59
40	160	1	2	-.33	2	5	-.43	12	3	.60	29	10	.49
40	180	0	7	-1.00	4	10	-.43	14	4	.56	27	16	.26
40	200	3	11	-.57	9	12	-.14	14	5	.47	26	17	.21
40	220	3	12	-.60	13	13	0	13	5	.44	29	15	.32
40	240	5	5	0	16	13	.10	9	5	.29	34	13	.45
40	260	8	0	1.00	12	11	.04	4	4	0	34	8	.62
40	280	8	0	1.00	13	10	.13	2	3	-.20	26	11	.41
40	300	8	0	1.00	12	7	.26	1	5	-.67	26	12	.37
40	320	7	0	1.00	15	8	.30	5	6	-.09	26	12	.37
40	340	7	2	.56	14	8	.27	5	5	0	28	14	.33
60	0	0	3	-1.00	5	3	.25	8	6	.14	11	10	.05
60	30	0	3	-1.00	3	0	1.00	9	5	.29	27	10	.19
60	60	0	3	-1.00	2	0	1.00	9	3	.50	28	10	.21
60	90	0	4	-1.00	0	0	/	8	2	.60	44	11	.60
60	120	0	2	-1.00	0	1	-1.00	9	2	.64	52	12	.63
60	150	0	1	-1.00	0	2	-1.00	12	3	.60	38	13	.49
60	180	0	0	/	0	4	-1.00	14	5	.47	23	12	.31
60	210	1	0	1.00	3	6	-.33	13	5	.44	20	15	.14
60	240	1	0	1.00	4	8	-.33	11	5	.38	11	13	-.08
60	270	2	0	1.00	4	6	-.20	7	4	.27	7	9	-.13
60	300	5	1	.67	5	6	-.09	5	5	0	7	9	-.13
60	330	4	1	.60	6	3	.33	7	6	.08	4	8	-.33
80	0	0	2	-1.00	1	2	-.33	9	4	.38	5	6	-.09
80	90	0	2	-1.00	0	1	-1.00	9	2	.64	37	10	.57
80	180	0	2	-1.00	0	2	-1.00	10	4	.43	20	12	.25
80	270	0	1	-1.00	1	4	-.60	8	4	.33	2	7	-.56

distance 45° from a point (δ, ϕ) on the focal sphere and the parameter k .

Area		5			6			7			8		
δ	ϕ	N_+	N_-	k	N_+	N_-	k	N_+	N_-	k	N_+	N_-	k
0	0	19	5	.58	19	7	.46	7	2	.56	20	12	.25
0	20	15	5	.50	28	16	.27	5	2	.43	20	9	.38
0	40	17	8	.36	29	18	.23	2	3	-.20	15	10	.20
0	60	15	10	.20	26	15	.27	5	3	.25	13	11	.08
0	80	21	10	.35	31	18	.27	8	3	.45	9	14	-.22
0	100	22	9	.42	30	12	.43	13	3	.63	11	12	-.04
0	120	25	6	.61	28	10	.47	19	2	.81	16	11	.19
0	140	31	7	.63	24	9	.45	16	3	.68	17	10	.26
0	160	23	5	.64	16	5	.52	9	3	.50	21	12	.27
20	0	20	5	.60	20	16	.11	14	2	.75	19	7	.46
20	20	15	7	.36	20	20	0	7	2	.56	19	8	.41
20	40	11	12	.04	26	21	.11	2	3	-.20	17	11	.21
20	60	12	12	0	24	21	.07	0	4	-1.00	13	12	.04
20	80	21	15	.17	20	21	-.02	3	2	.20	9	14	-.22
20	100	22	12	.29	20	16	.11	6	1	.71	12	16	-.14
20	120	18	9	.33	18	10	.29	6	3	.33	15	13	.07
20	140	25	5	.67	12	11	.04	3	5	-.25	18	11	.24
20	160	21	7	.50	9	9	0	2	7	-.56	20	11	.29
20	180	15	4	.58	17	6	.48	3	6	-.33	20	11	.29
20	200	11	4	.47	30	13	.40	1	7	-.75	19	7	.46
20	220	13	5	.44	33	14	.40	3	8	-.45	15	10	.20
20	240	12	5	.41	35	12	.49	10	7	.18	12	9	.14
20	260	18	5	.57	48	12	.60	14	7	.33	8	8	0
20	280	23	3	.77	39	10	.59	20	6	.54	10	8	.11
20	300	22	3	.76	31	8	.59	22	4	.69	14	9	.22
20	320	24	4	.71	29	9	.53	23	2	.84	17	9	.31
20	340	22	5	.63	26	17	.21	19	2	.81	21	9	.40
40	0	19	5	.58	20	19	.03	17	5	.55	10	2	.67
40	20	11	8	.16	20	23	-.07	12	5	.41	12	6	.33
40	40	6	10	-.25	16	22	-.16	6	5	.09	9	6	.20
40	60	10	14	-.17	13	22	-.26	3	6	-.33	6	8	-.14
40	80	13	14	-.04	8	21	-.45	1	8	-.78	7	9	-.13
40	100	14	11	.12	6	14	-.40	1	9	-.80	5	11	-.38
40	120	12	9	.14	6	13	-.37	1	9	-.80	7	12	-.26
40	140	12	6	.33	5	13	-.44	1	10	-.82	9	11	-.10
40	160	14	5	.47	2	13	-.73	1	10	-.82	9	10	-.05
40	180	12	2	.71	15	8	.30	1	12	-.85	12	9	.14
40	200	8	1	.78	25	8	.52	2	12	-.71	12	6	.33
40	220	8	3	.45	28	12	.40	4	13	-.53	9	3	.50
40	240	12	5	.41	35	13	.46	11	11	0	5	4	.11
40	260	16	4	.60	49	11	.63	19	11	.27	3	3	0
40	280	21	3	.75	44	9	.66	24	9	.45	6	4	.20
40	300	20	2	.82	35	12	.49	28	6	.65	8	1	.78
40	320	17	4	.62	34	12	.48	27	5	.69	12	2	.71
40	340	15	5	.50	26	17	.21	22	5	.63	11	1	.83
60	0	9	4	.38	15	17	-.06	19	11	.27	1	0	1.00
60	30	5	9	-.29	14	21	-.20	11	9	.10	2	2	0
60	60	9	10	-.05	11	24	-.37	7	10	-.18	2	3	-.20
60	90	10	10	/	7	19	-.46	4	13	-.53	2	3	-.20
60	120	8	9	-.06	5	15	-.50	3	16	-.68	3	4	-.14
60	150	7	5	.17	11	12	-.04	3	16	-.68	3	5	-.25
60	180	5	1	.67	14	12	.08	5	17	-.55	0	0	/
60	210	4	1	.60	22	6	.57	5	18	-.57	0	0	/
60	240	7	1	.75	28	9	.51	12	18	-.20	1	0	1.00
60	270	7	1	.75	32	10	.52	22	15	.19	1	0	1.00
60	300	10	2	.67	29	13	.38	25	13	.32	1	0	1.00
60	330	10	4	.43	24	16	.20	22	12	.29	1	0	1.00
80	0	1	3	-.50	15	18	-.09	12	16	-.14	1	0	1.00
80	90	2	6	-.50	13	20	-.21	8	17	-.36	2	3	-.20
80	180	2	3	-.20	14	13	.04	6	19	-.52	0	0	/
80	270	1	2	-.33	18	16	.06	13	18	-.16	1	0	1.00

(to be continued)

Area		9			10			11			12		
δ	φ	N_+	N_-	k	N_+	N_-	k	N_+	N_-	k	N_+	N_-	k
0	0	8	1	.78	6	17	-.48	12	10	.09	5	14	-.47
0	20	15	2	.76	6	19	-.52	11	8	.16	11	21	-.31
0	40	15	5	.50	5	20	-.60	14	9	.22	19	24	-.12
0	60	11	7	.22	9	19	-.36	16	6	.05	24	17	.17
0	80	4	6	-.20	13	10	-.13	17	5	.05	28	10	.47
0	100	1	6	-.71	18	5	.57	22	5	.63	27	2	.86
0	120	0	5	-1.00	20	6	.54	21	4	.68	23	3	.77
0	140	1	3	-.50	18	6	.50	16	3	.68	14	7	.33
0	160	2	1	.33	14	8	.27	11	9	.10	9	11	-.10
20	0	21	9	.40	8	16	-.33	12	8	.20	10	16	-.23
20	20	25	5	.67	5	20	-.60	9	9	0	14	19	-.15
20	40	28	5	.70	5	21	-.62	12	5	.41	23	19	.10
20	60	28	6	.65	5	18	-.57	12	2	.71	24	10	.41
20	80	21	5	.62	10	11	-.05	8	1	.78	24	4	.71
20	100	8	4	.33	15	4	.58	8	1	.78	21	1	.91
20	120	5	0	1.00	15	3	.67	9	1	.80	18	1	.89
20	140	5	0	1.00	14	5	.47	9	3	.50	12	3	.60
20	160	2	0	1.00	10	7	.18	7	6	.08	5	8	-.23
20	180	1	0	1.00	8	11	-.16	13	9	.18	3	13	-.62
20	200	3	0	1.00	5	19	-.58	14	10	.17	6	22	-.57
20	220	3	2	.20	5	19	-.58	16	9	.28	11	20	-.29
20	240	1	5	-.67	9	14	-.22	21	8	.45	19	17	.06
20	260	1	9	-.80	15	11	-.15	26	8	.53	30	16	.30
20	280	1	13	-.86	21	8	.45	27	7	.59	29	9	.53
20	300	1	15	-.88	22	3	.76	27	7	.59	23	4	.70
20	320	0	13	-1.00	20	7	.48	24	7	.55	21	9	.40
20	340	6	10	-.25	14	10	.17	18	10	.29	15	15	0
40	0	28	16	.27	8	12	-.20	14	6	.40	16	16	0
40	20	29	13	.38	4	11	-.47	9	5	.29	16	14	.07
40	40	31	9	.55	4	10	-.43	4	4	0	21	13	.24
40	60	33	5	.74	4	12	-.50	2	0	1.00	23	8	.48
40	80	28	5	.70	6	8	-.14	2	0	1.00	22	5	.63
40	100	17	4	.62	7	4	.27	2	1	.33	19	0	1.00
40	120	9	0	1.00	9	3	.50	3	1	.50	10	0	1.00
40	140	6	0	1.00	6	4	.20	1	3	-.50	4	0	1.00
40	160	6	0	1.00	6	3	.33	1	4	-.60	2	3	-.20
40	180	4	0	1.00	5	7	-.17	5	7	-.17	0	8	-1.00
40	200	2	1	.33	4	10	-.43	7	9	-.13	5	14	-.47
40	220	2	7	-.56	5	10	-.33	13	9	.18	9	15	-.25
40	240	2	13	-.73	8	12	-.20	21	8	.45	16	16	0
40	260	2	16	-.78	14	8	.27	26	8	.53	19	15	.12
40	280	2	21	-.83	16	3	.68	29	7	.61	23	11	.35
40	300	1	21	-.91	16	5	.52	23	6	.59	24	9	.45
40	320	5	19	-.58	14	5	.47	25	5	.67	20	9	.38
40	340	15	18	-.09	10	8	.11	21	6	.56	17	14	.10
60	0	28	21	.14	7	7	0	9	5	.29	14	6	.40
60	30	32	18	.28	4	7	-.27	2	2	0	13	7	.30
60	60	32	11	.49	1	4	-.60	0	0	/	15	7	.36
60	90	26	7	.58	2	3	-.20	0	0	/	16	2	.78
60	120	16	3	.68	2	1	.33	0	0	/	8	0	1.00
60	150	10	2	.67	3	1	.50	0	1	-1.00	3	1	.50
60	180	6	4	.20	3	2	.20	2	3	-.20	2	9	-.64
60	210	3	10	-.54	5	2	.43	7	5	.17	7	12	-.26
60	240	2	17	-.79	5	3	.25	19	7	.46	15	13	.07
60	270	2	21	-.83	10	3	.54	18	7	.44	15	12	.11
60	300	8	22	-.47	9	4	.39	18	7	.44	15	11	.15
60	330	18	20	-.05	8	6	.14	16	6	.45	14	6	.40
80	0	22	18	.10	6	5	.09	8	3	.45	10	6	.25
80	90	21	14	.20	1	3	-.50	0	0	/	12	2	.71
80	180	13	13	0	2	1	.33	2	1	.33	2	7	-.56
80	270	14	18	-.13	8	3	.45	18	6	.50	15	12	.11

(continued)

Area		13			14			15			16		
δ	φ	N_+	N_-	k	N_+	N_-	k	N_+	N_-	k	N_+	N_-	k
0	0	4	19	-.65	14	14	0	6	14	-.40	2	12	-.71
0	20	8	10	-.11	13	17	-.13	11	13	-.08	0	16	-1.00
0	40	21	10	.35	12	20	-.25	11	12	-.04	1	10	-.82
0	60	27	12	.38	10	16	-.23	12	12	0	1	10	-.82
0	80	32	7	.64	10	9	.05	14	10	.17	1	8	-.78
0	100	22	6	.57	10	12	-.09	6	9	-.20	1	1	0
0	120	13	13	0	10	12	-.09	4	14	-.56	1	5	-.67
0	140	8	16	-.33	10	11	-.05	3	15	-.67	1	6	-.71
0	160	3	16	-.68	14	14	0	2	13	-.73	2	7	-.56
20	0	4	17	-.62	13	14	-.04	3	13	-.63	4	15	-.58
20	20	11	12	-.04	13	14	-.04	9	11	-.10	4	17	-.62
20	40	17	11	.21	16	15	.03	11	12	-.04	2	13	-.73
20	60	20	10	.33	11	16	-.19	12	10	.09	1	11	-.83
20	80	22	4	.69	8	10	-.11	10	9	.05	1	8	-.78
20	100	18	5	.57	11	8	.16	3	10	-.54	1	3	-.50
20	120	13	12	.04	10	10	0	4	14	-.56	0	2	-1.00
20	140	8	13	-.24	9	10	-.05	3	13	-.63	0	5	-1.00
20	160	4	13	-.53	8	10	-.11	2	15	-.76	0	6	-1.00
20	180	1	17	-.89	8	14	-.27	5	16	-.52	0	6	-1.00
20	200	12	11	.04	10	17	-.26	11	12	-.04	0	7	-1.00
20	220	19	10	.31	9	19	-.36	11	11	0	0	9	-1.00
20	240	23	10	.39	10	15	-.20	12	10	.09	1	7	-.75
20	260	27	5	.69	9	13	-.18	13	9	.18	2	3	-.20
20	280	26	7	.58	9	11	-.10	5	6	-.09	3	2	.20
20	300	15	14	.03	8	10	-.11	4	10	-.43	4	7	-.27
20	320	9	14	-.22	13	8	-.24	3	11	-.57	5	8	-.23
20	340	6	13	-.37	13	14	-.04	1	11	-.83	6	11	-.29
40	0	6	10	-.25	11	11	0	0	6	-1.00	0	7	-.30
40	20	8	10	-.11	11	13	-.08	1	4	-.60	6	18	-.50
40	40	12	9	.14	14	13	.04	3	6	-.33	5	15	-.50
40	60	18	3	.71	7	9	-.13	2	6	-.50	3	14	-.65
40	80	15	3	.67	6	7	-.07	1	5	-.67	1	11	-.83
40	100	14	5	.47	7	5	.17	3	7	-.40	1	4	-.60
40	120	11	8	.16	6	6	0	3	8	-.45	0	2	-1.00
40	140	7	10	-.18	7	4	.27	3	11	-.57	0	4	-1.00
40	160	2	8	-.60	4	6	-.20	1	10	-.82	0	5	-1.00
40	180	3	7	-.40	3	7	-.40	1	11	-.83	0	4	-1.00
40	200	11	11	0	6	10	-.25	9	10	-.05	0	4	-1.00
40	220	17	8	.36	4	10	-.43	11	9	.10	0	4	-1.00
40	240	21	5	.62	5	7	-.17	10	8	.11	1	3	-.50
40	260	23	5	.64	6	10	-.25	9	5	.29	2	2	0
40	280	20	5	.60	6	11	-.29	2	4	-.33	3	3	0
40	300	16	11	.19	8	9	-.06	2	6	-.50	6	6	0
40	320	6	12	-.33	9	8	.60	1	9	-.80	7	10	-.18
40	340	4	11	-.47	10	9	.05	1	7	-.75	7	12	-.26
60	0	6	4	.20	7	3	.40	0	2	-1.00	7	9	-.13
60	30	10	4	.43	9	2	.64	0	2	-1.00	5	12	-.41
60	60	10	2	.67	4	3	.14	0	3	-1.00	4	13	-.53
60	90	9	3	.50	5	5	0	0	6	-1.00	3	7	-.40
60	120	7	5	.17	3	4	-.14	0	5	-1.00	0	6	-1.00
60	150	4	3	.14	3	5	-.25	0	5	-1.00	0	5	-1.00
60	180	5	3	.25	2	3	-.20	0	5	-1.00	0	5	-1.00
60	210	11	4	.47	3	4	-.14	0	3	-1.00	0	5	-1.00
60	240	15	4	.58	2	6	-.50	0	1	-1.00	3	6	-.33
60	270	14	4	.56	0	5	-1.00	0	1	-1.00	3	5	-.25
60	300	11	6	.29	4	5	-.11	0	1	-1.00	7	4	.27
60	330	5	5	0	6	5	-.09	0	1	-1.00	7	10	-.18
80	0	3	1	.50	5	2	.42	0	1	-1.00	6	8	-.14
80	90	6	3	.33	4	0	1.00	0	6	-1.00	3	7	-.40
80	180	0	2	-1.00	2	3	-.20	0	4	-1.00	3	6	-.33
80	270	11	2	6.9	0	3	-1.00	0	0	/	5	6	-.09

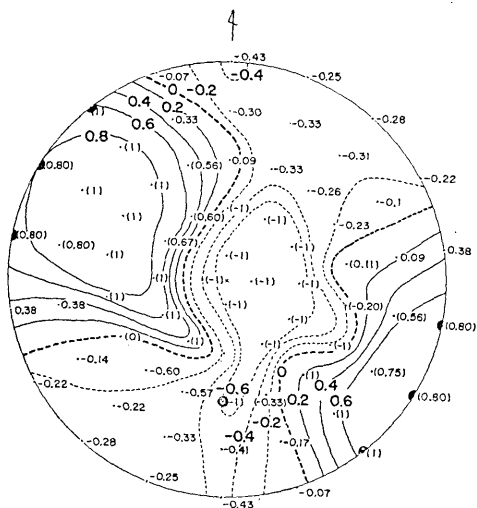


Fig. 3. An example of plotted k values and lines of equal k . (The values in the bracket are obtained from data with the size smaller than 10.) The upper hemi-focal sphere is projected in such a way that the radial distance is proportional to the angle from the vertical.

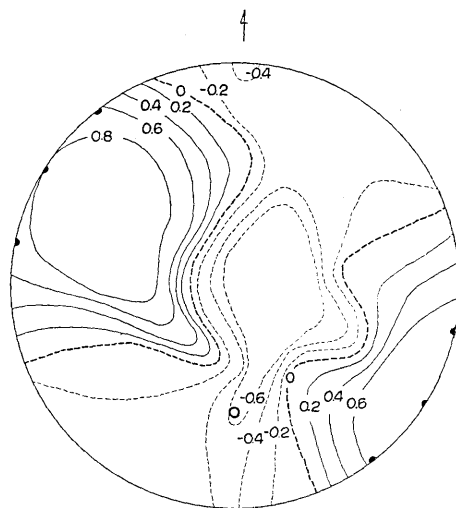


Fig. 4. Equal lines of the k values for Area 1 (Urakawa-Oki).

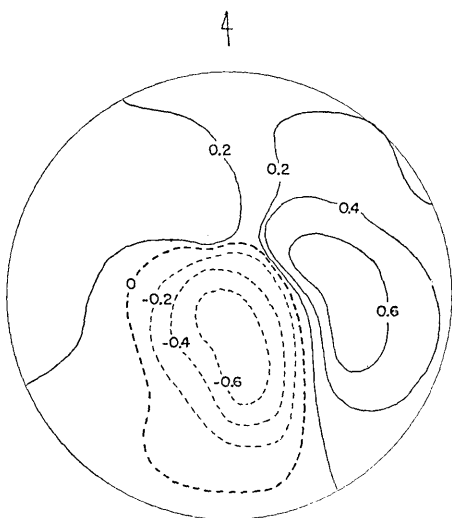


Fig. 5. Equal lines of the k values for Area 2 (Miyagi-Oki).

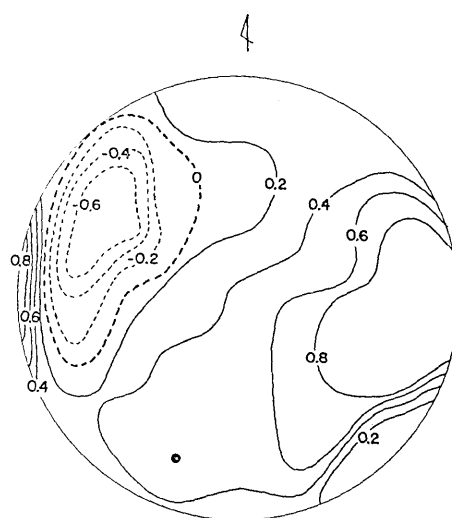


Fig. 6. Equal lines of the k values for Area 3 (intermediate earthquakes in Tohoku).

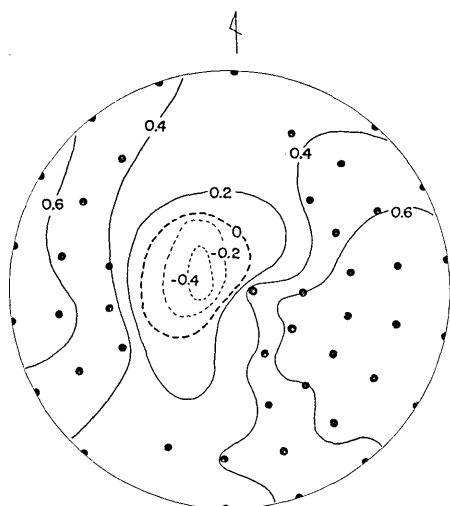


Fig. 7. Equal lines of the k values for Area 4 (Fukushima-Ibaragi-Oki).

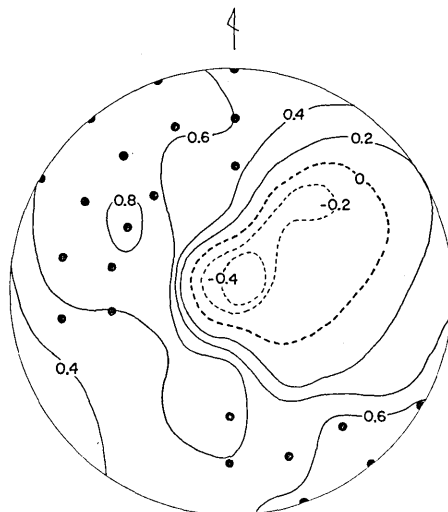


Fig. 8. Equal lines of the k values for Area 5 (Chiba-Oki).

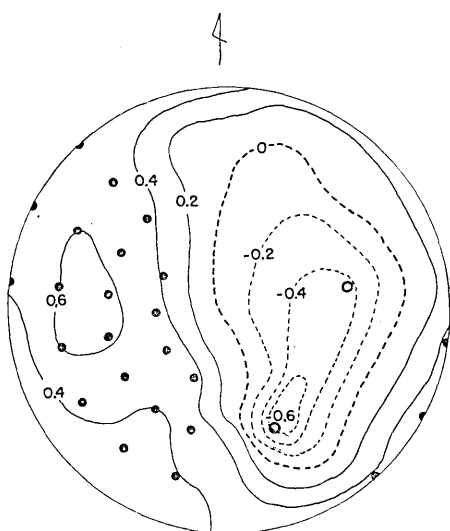


Fig. 9. Equal lines of the k values for Area 6 (south-west of Ibaragi).

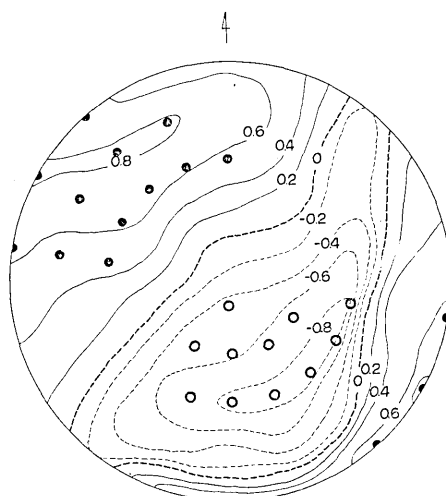


Fig. 10. Equal lines of the k values for Area 7 (intermediate earthquakes in southern Kanto).

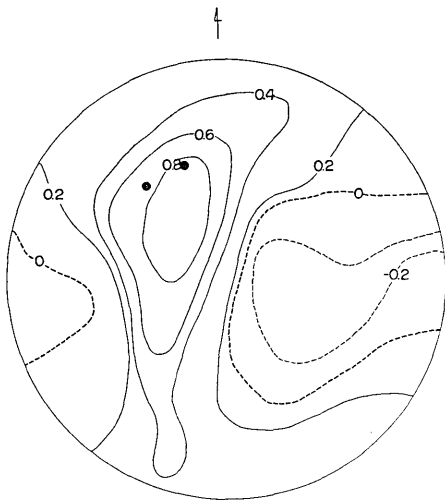


Fig. 11. Equal lines of the k values for Area 8 (western Kanagawa).

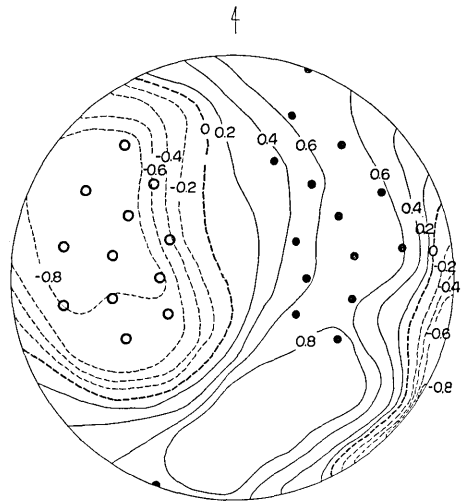


Fig. 12. Equal lines of the k values for Area 9 (deep earthquakes in Chubu).

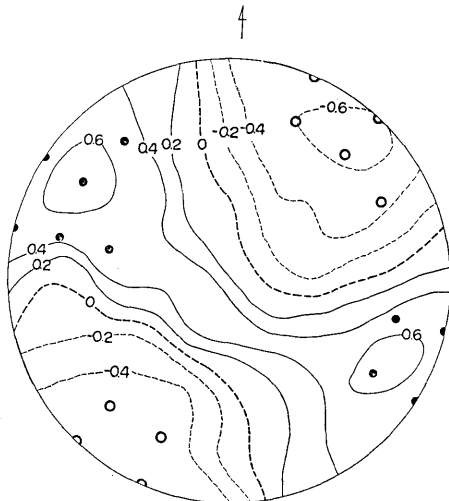


Fig. 13. Equal lines of the k values for Area 10 (Hida-Akaishi mountains).

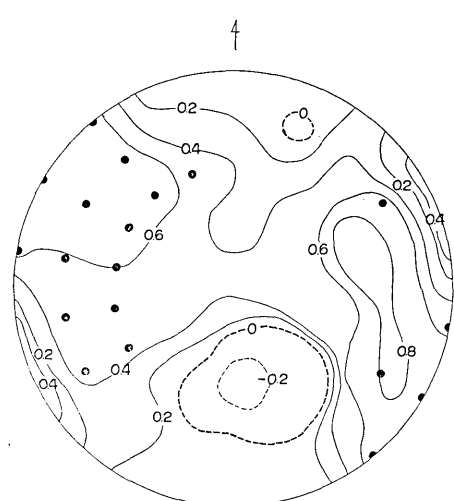


Fig. 14. Equal lines of the k values for Area 11 (Hakusan mountains).

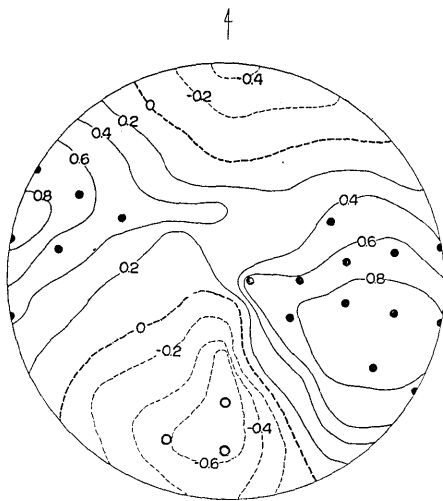


Fig. 15. Equal lines of the k values for Area 12 (Echizen-Misaki-Oki).

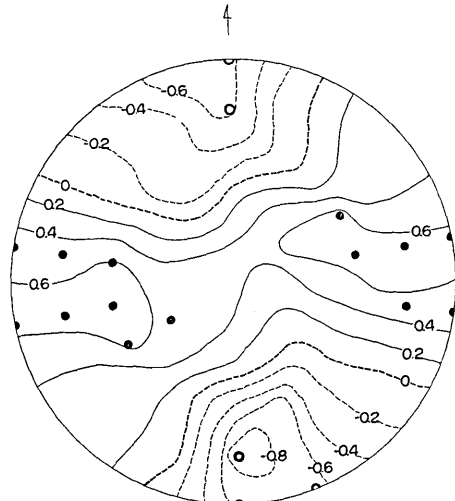


Fig. 16. Equal lines of the k values for Area 13 (western Hyogo).

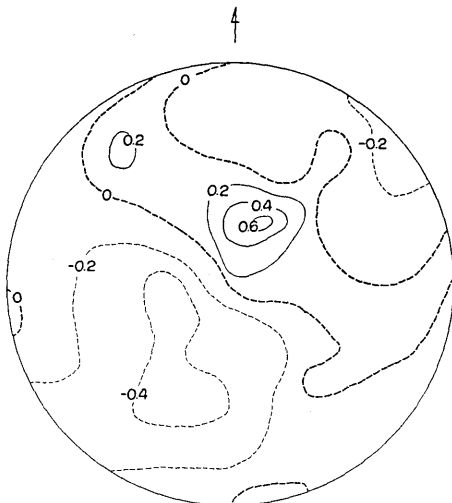


Fig. 17. Equal lines of the k values for Area 14 (Kii-Suido).

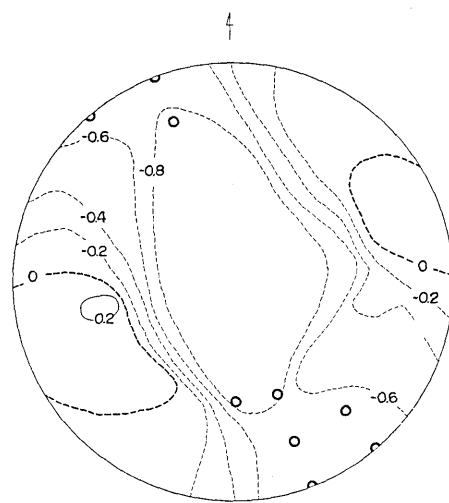


Fig. 18. Equal lines of the k values for Area 15 (Miyazaki-Oki).

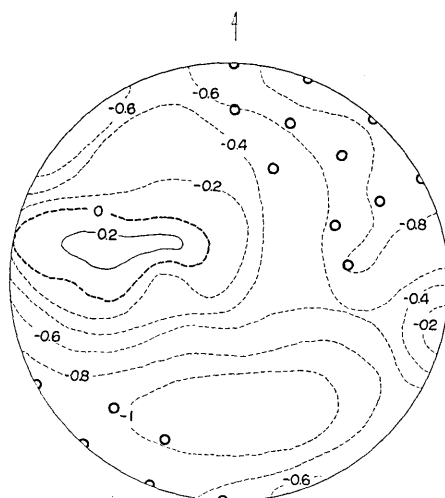


Fig. 19. Equal lines of the k values for Area 16 (intermediate earthquakes in southern Kyushu).

§ 5. Types of the smoothed radiation patterns

The maximum of the parameter k on a focal sphere corresponding to an area indicates the direction in which the seismic sources in the area radiate *dilatations* most frequently. Using the nomenclature in the *fault plane* seismology,¹³⁾ we shall call it the direction of *axis of maximum pressure*. The minimum of the parameter k corresponds to the *axis of maximum tension*.

The actual patterns of equal k lines as shown in Fig. 4 through Fig. 19 suggest that we may classify the patterns into the following three types according to the directions of the above two axes.

Type *Q*: Both axes lie nearly horizontally. This type corresponds to a strike-slip movement on a vertical fault. The pattern of first motions plotted on a map of stations will show the familiar quadrant pattern, this being classified as *Q*-type by some Japanese seismologists.

Type *P*: The axis of maximum pressure lies nearly horizontally, but the axis of maximum tension is directed nearly vertically. This type corresponds to a reverse dip-slip movement along an inclined fault. The naming of this type follows Ritsema.¹⁴⁾

Type *I*: Both axes are *inclined*. This type roughly corresponds

13) H. HONDA, *loc. cit.*, 1).

14) A. R. RITSEMA, *Geophys. Jour. Roy. Astro. Soc.*, 3 (1960), 307-313.

to either a horizontal movement along a horizontal fault or a vertical movement along a vertical fault.

Schematic pictures of the patterns of equal k for these types are shown in Fig. 20. As will be described later, type Q prevails in the

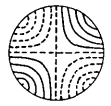
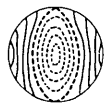

Type	schematic lines of equal k	axis max. pressure	axis max. tension	fault model	area
Q		horizontal	horizontal	strike-slip along vertical fault	inland crust
P		horizontal	vertical	reverse dip-slip along inclined fault	off coast crust uppermost mantle
I		inclined	inclined	vertical slip along vertical fault or horizontal slip along horizontal fault	deep intermediate earthquake zone

Fig. 20. Three types of k value pattern and their prevailing areas.

crust of inland areas, type P in the areas off the Pacific coast, and type I in between the above two regions as well as in the deep-intermediate earthquake zone.

According to our classification based on the orientation of pressure and tension axes, one other type is possible, that has a horizontal tension and a vertical pressure axis corresponding to a normal dip-slip along an inclined fault (an extreme case of type T of Ritsema). We find, however, no such type in Japan, except for Area 14 where the pressure axis seems to incline a little steeper than the tension axis.

§ 6. Discussion of the result

There is a remarkable similarity in the pattern of equal k lines between areas of a similar geographical situation. The pattern shows type Q for the inland crust in central and western Japan (Area 10, 11, 12 and 13). We find type P in the crust and uppermost mantle in the ocean off the Pacific coast (Area 1, 2, 4, 5 and 15). On the other hand, type I prevails in the crust and uppermost mantle inland near the Pacific coast (Area 6, 8) as well as in the intermediate-deep earthquake zone (Area 3, 7, 9 and 16).

In other words, the pressure axis lies nearly horizontally in the crust inland as well as in the ocean off the Pacific coast. On the other

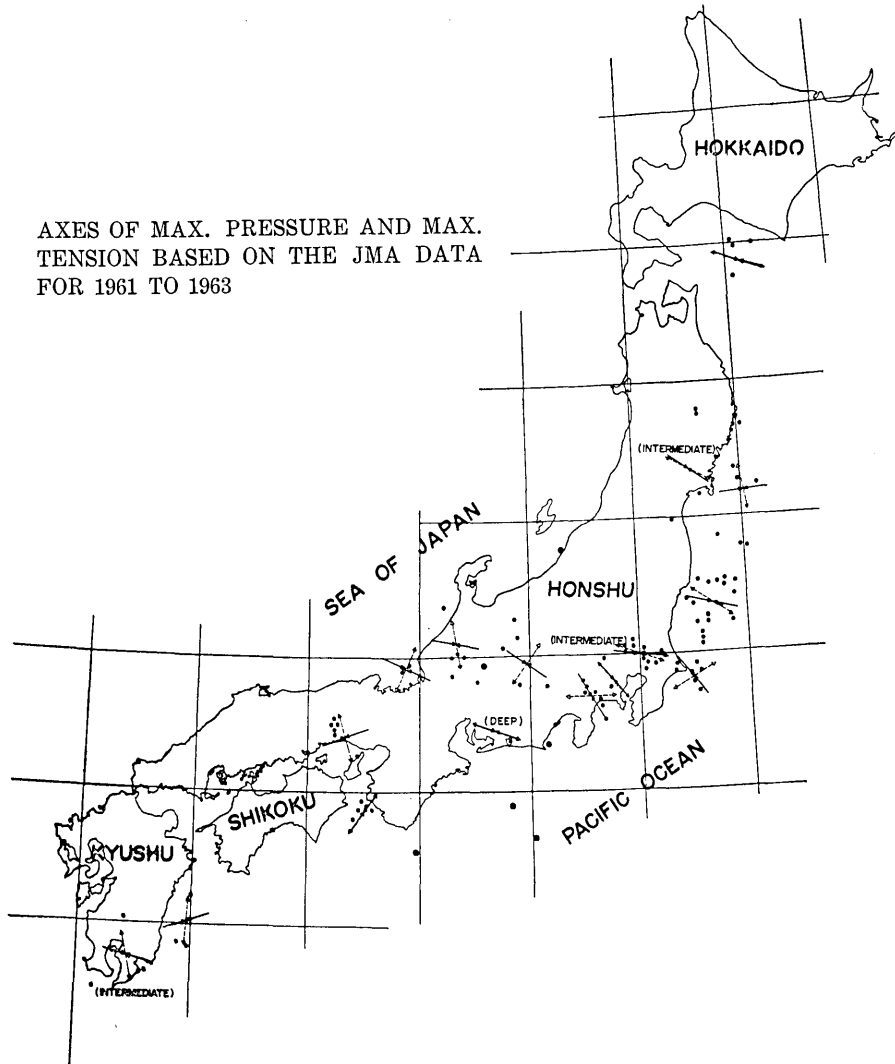


Fig. 21. The average azimuths of the axes of maximum pressure and maximum tension are shown by arrows roughly at the centre of epicentres (dots) of earthquakes over which the average is taken. The pressure axis shows more systematic geographic distribution than the tension axis. The pressure axis lies roughly in the NWW-SEE direction in eastern and central Japan (perpendicular to the trend of Honshu), while it lies in the NEE-SWW direction in western Japan (parallel to the trend).

hand, the tension axis lies nearly horizontally in the crust inland, but tends to be directed vertically in the ocean off the Pacific coast. Both axes are inclined in between the above two regions and in the regions in the intermediate-deep earthquake zone.

The azimuths of the maximum pressure and tension axes are read

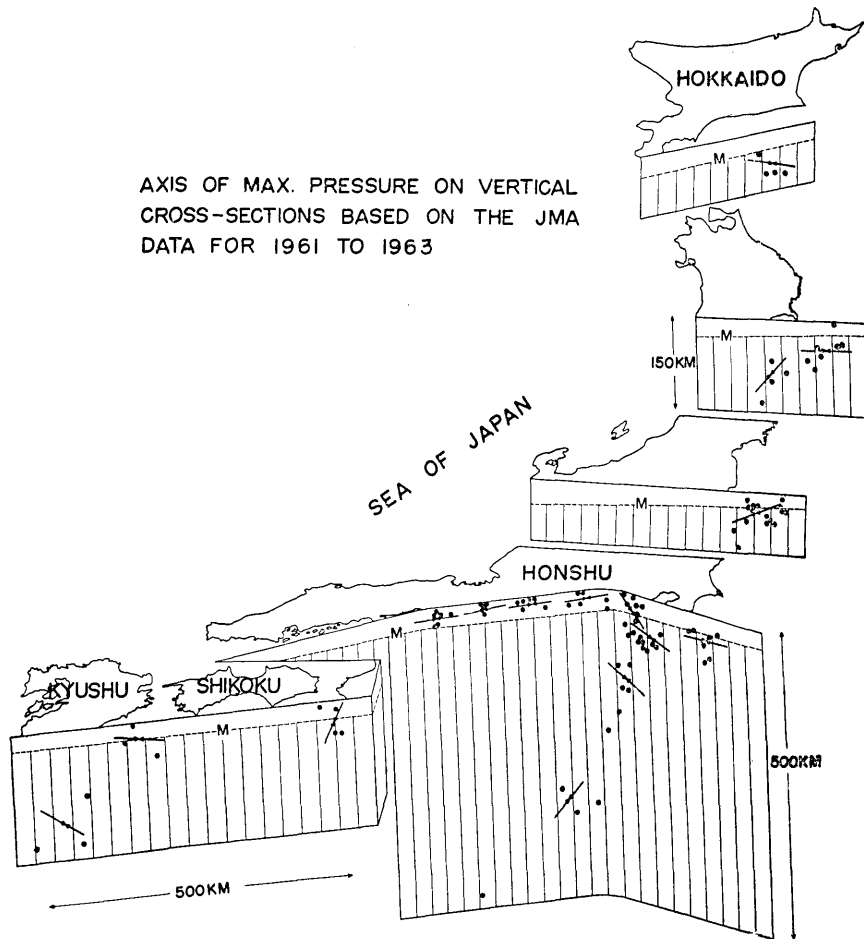


Fig. 22. The average orientation of the maximum pressure axis is shown, by arrows roughly at the centre of hypocentres (dots) of earthquakes over which the average is taken, in vertical cross-sections cut roughly parallel to the azimuth of the axis. The axis lies nearly horizontally in the inland crust as well as in the crust and uppermost mantle under the ocean off the Pacific coast. It is inclined in between the above two regions as well as in the intermediate-deep earthquake zone.

from the pattern of equal k values, and are shown on a map in Fig. 21. The azimuth of pressure axis shows more systematic geographical distribution than that of tension axis. The pressure axis tends to lie perpendicular to the trend of the Honshu island in north-eastern Japan, and parallel to that in south-western Japan.

Fig. 22 shows the orientation of the pressure axis in vertical cross-sections cut roughly parallel to the azimuth of the axis. As mentioned before, the axis lies nearly horizontally in the inland crust as well as in the crust and uppermost mantle under the ocean off the Pacific coast. It is inclined one way or the other in between the above two regions as well as in the intermediate-deep earthquake zone.

All the results mentioned above are in surprisingly good agreement with the results obtained by Honda¹⁵⁾ and his colleagues and Ichikawa¹⁶⁾ from the data on major earthquakes which have occurred in Japan during the last 40 years. This agreement between the result from a short-term small earthquake data and those from a long-term large earthquake data suggests an existence of persistent regional stress field throughout the crust and upper-mantle in Japan. As demonstrated in Figs. 21 and 22, such a regional stress field may be generated by a compressive force exerted roughly in the NWW-SEE direction in eastern and central Japan, and in the NEE-SWW direction in western Japan. The fact that the pressure axis lies nearly horizontal in the inland crust and under the ocean off the Pacific coast, but is inclined in between the above two regions may imply that the above-mentioned compressive force is not produced by a distant agent outside of Japan, but by an agent inside of Japan, perhaps in the area of inclined pressure axis. This area is where the largest earthquakes in Japan, such as the Kanto earthquake of 1923 and the Nankaido earthquake of 1946, take place. Matsuzawa¹⁷⁾ postulated growth of a magma pocket located at the uppermost mantle beneath the epicentral area as the cause of these largest of earthquakes. Such an expanding nucleus may account for the orientation of the pressure axis in the entire area of Japan such as shown in Fig. 22 including the deep earthquake zone. We may further speculate on the supply of material and energy for the growth of the magma pocket by taking into account recent findings on the upper-mantle structure.

Accumulating evidences from surface wave data support a signifi-

15) H. HONDA, *loc. cit.*, 1).

16) M. ICHIKAWA, *Geophys. Mag.*, (in press).

17) T. MATUZAWA, *Study of Earthquakes* (Tokyo, 1964), p. 196.

cant difference in the nature of the asthenosphere low velocity channel between oceans, shields and orogenic area.¹⁸⁾ The shear velocity in the channel seems lower in the ocean than in the shield area. In other words, the evidence of the channel is more pronounced in the ocean. Further, the top of the channel seems shallower in the ocean than in the shield. In an orogenic area like Japan, the shear velocity in the uppermost mantle is as low as that in the channel in the ocean, and it seems as if the channel reaches the *M* discontinuity in the orogenic area.¹⁹⁾

Japan is located at the boundary of the Pacific ocean and Eurasian continent. If the above-mentioned difference in low velocity channel is real, the low velocity channel of the ocean must be blocked by the high velocity mantle of the continent at this boundary. If the channel includes patches of magma, it seems likely that the magma is squeezed out of the channel at this boundary and forms an expanding magma pocket responsible for earthquake generating stress. The magma pocket may be formed at the crossing of the upper boundary of the low velocity channel (depth of about 80 km) and the deep-intermediate earthquake zone which is often regarded as the boundary of oceanic mantle and continental mantle. This location of the expanding nucleus seems most adequate for explaining the orientation of the maximum pressure axis in the entire area of Japan.

Appendix: A test of significance

If all the earthquakes in a group occur with an identical orientation of nodal planes, the *k* value will take +1 somewhere on the focal sphere. The variability of the orientation of the planes among earthquakes as well as the presence of noises on seismograms, however, will reduce this maximum value. We shall consider an extreme case, where the orientation is purely random, and *compressions* and *dilatations* occur with the same probability 1/2 in any area of the focal sphere.

The probability that the *k* value exceeds *k*₀ is equal to the probability that the number *N*₊ of dilations exceeds the largest integer *N*₀ less than $(1+k_0)n/2$, where *n* is the sum of *N*₊ and *N*₋. For the random case, the above probability is given by a binomial series,

$$\begin{aligned} Pr(k > k_0) &= Pr(N_+ > N_0) \\ &= 1 - \sum_{r=0}^{N_0} \frac{n!}{(n-r)!r!} \left(\frac{1}{2}\right)^n. \end{aligned}$$

18) J. BRUNE and J. DORMAN, *Bull. Seis. Soc. Am.*, **53** (1963), 167-210.

19) K. AKI, *Trans. Amer. Geophys. Union*, **44** (1963), 807-811.

In finding the direction of the axis of maximum pressure, we look for the maximum of k value on the focal sphere. If there are m independent measurements of k for one focal sphere, the probability that the maximum of k exceeds k_0 will be

$$Pr(\max. k > k_0) = 1 - \left(\sum_{r=0}^{N_0} \frac{n!}{(n-r)!r!} \left(\frac{1}{2}\right)^n \right)^m.$$

The number m of independent measurements of k may be taken as the ratio of the total area of sphere to the area occupied by a single measurement of k , that is, the area within an angular distance of 45° from a point and its antipode on the surface of sphere. The ratio is $1/(1-1/\sqrt{2})=3.414$. Permitting a small overlapping of the independent areas, we shall take $m=4$ as the number of independent measurements of k .

Taking $m=4$, we determined the value of k_0 , for which

$$Pr(\max. k > k_0) = 0.05,$$

and plotted the value against the sum n of the numbers of *compressions* and those of *dilations* as shown in Fig. 23. For example, if $n=20$, the probability that the maximum of k exceeds about 0.55 is 5%. If the observed maximum value of k exceeds this limit, we may state that the randomness of the radiation pattern is rejected on the significance level of 5%.

The same criterion applies to the maximum of negative k value which corresponds to the axis of maximum tension.

The positions on the focal sphere where the absolute values of k exceed the above limit are indicated in Figs. 4 to 19 by closed circles for positive k and by open circles for negative k . Except for Area 2 and 14, the significantly large $|k|$ values are observed at some points on the focal sphere.

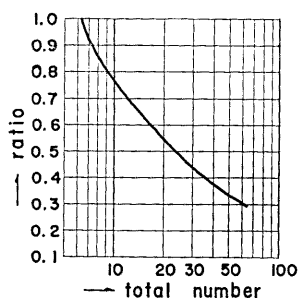


Fig. 23. The limit of the maximum of the k value on the significance level of 5%, as plotted against the sample size.

25. 昭和 36~38 年における本邦各地の平均的発震機構

地震研究所 安芸敬一

ある地域に働く平均的な起震力を、できるだけ客観的に求める試みとして、次のような方法を考えた。まず、現在の段階でもつともらしいと思われる地殻構造を基に、気象庁地震月報の *ip* のデータを用いて、震源の深さを決め直し、同時に各観測点への射出角を求める。次に注目する地域内の地震の全体を 1 つの地震のように見做して、その地震の震源球上での押し引き分布を Wulff の net によつて投影する。この仮想震源球上にある点 Q とその antipode Q' をとり、これらの点から角距離 45 度以内の押しの数と引きの数を算え、これらの数の差と和の比を k 値と呼ぶ。 k はもしすべて押しなら -1 、すべて引きなら $+1$ 、押し引きが同じ数なら 0 になる。 Q 点を球面上いろいろの場所にとって k の値を求め、それを対応する点 Q のところに plot し、等 k 値線を引くと、その結果はいわば normalize され smoothing された P 波初動分布を与える。

こうして得られた等 k 値線の模様型が著しい地域性を示す。いわゆる 4 象限型、つまり断層模型としては垂直な断層面に沿う水平方向の迂りとなる型は中部地方および西日本の地殻内地震に見られる。これに対して、傾いた断層面に沿う上下方向の迂りに対応する型は関東・東北地方沖の太平洋に見られる。しかもこれらは逆断層型である。これら 2 つの地域では、主圧力の軸は水平方向に近いが、この中間の地域では主圧力も主張力の軸も深発地震同様に傾いているように見える。

われわれの結果は、僅か 30 ヶ月のデータに基づくものであるが、過去 40 年の多くの地震を扱った本多、市川らの結論とほとんど完全に一致している。このことは、主圧力の軸の方位が地理的な系統的分布をしていることと併せ考えると、ある定つた pattern の stress 状態が日本の地下に常に存在していることを示すように思われる。このような stress を生じるような原因となるものについて考えて見た。